ISSN 0027-1349, Moscow University Physics Bulletin, 2024, Vol. 79, Suppl. 2, pp. S700–S705. © Allerton Press, Inc., 2024.

Multidimensional Global Optimization of Detector Systems Using the Example of Muon Shield in the SHiP Experiment

E. O. Kurbatov[1,2*], F. D. Ratnikov[1,2], and E. D. Ursov[3***]**

[1] *HSE University, Moscow, 101000 Russia*
[2] *Yandex School of Data Analysis, Moscow, 119021 Russia*
[3] *Humboldt University of Berlin, Berlin, 12489 Germany*
Received October 1, 2024; revised October 10, 2024; accepted October 20, 2024

Abstract—SHiP (Search for Hidden Particles) is a new general-purpose experiment at the SPS ring at CERN, aimed at searching for hidden particles proposed by numerous theories beyond the Standard Model. An important element of the experiment is muon shield. On one hand, it must provide good background suppression, and on the other hand, it should not be too heavy. This work presents the results of obtaining muon shield configurations using Bayesian optimization with several types of surrogates. This allowed for effective global multidimensional optimization in a 42-dimensional space and reduced the muon flux by 2.5 times while maintaining the original mass of the shield.

Keywords: CERN, new physics, high energy physics, SHiP

DOI: 10.3103/S0027134924702151

1. INTRODUCTION

Search for Hidden Particles (SHiP) [1] is a new fixed-target experiment that will be located at the Super Proton Synchrotron (SPS) at CERN. The operational energy of the SPS is 400 GeV. The goal of the experiment is to search for hidden particles predicted by numerous Hidden Sector models, which can describe the distribution of dark matter in the Universe, neutrino oscillations, and baryon asymmetry in the Universe. The experiment is aimed at searching for new physics. The high sensitivity of the experiment to signals associated with particles beyond the Standard Model is achieved thanks to the high luminosity of the SPS and the large fluxes of produced charmed mesons and photons directed at the detector system due to the fixed target.

In 2022, a new version of SHiP was proposed to be shortened by 10 m and narrowed in transverse dimensions to fit into the SPS ECN3 hall [2], which currently houses the NA62 experiment [3]. This inevitably led to the problem of finding a new configuration for the muon shield to maintain the background level at an acceptable level.

2. SHIP EXPERIMENT

The Standard Model (SM) of elementary particles has proven its success in theoretically predicting experimental observations in high-energy physics [4]. However, it has several shortcomings related to the existence of dark matter and baryon asymmetry in the Universe [5]. Consequently, models of the Hidden Sector (beyond the SM) are actively being developed, introducing new weakly interacting particles that can address these issues. Given the absence of signals from new particles in the GeV—TeV mass range, numerous experiments have been directed towards searching for long-lived weakly interacting particles (FIPs) on the GeV scale. The most promising candidates include heavy neutral leptons (HNL), dark photons (DP), dark scalars (DS), axion-like particles (ALP), and light dark matter (LDM) [6, 7].

The primary goal of the currently developing SHiP (Search For Hidden Particles) experiment, a fixed-target experiment at the SPS facility (proton beam energy of 400 GeV) at CERN, is to search for hidden sector particles [1, 8]. For this purpose, SHiP will implement a detector system designed to register possible decay products or direct signals from new particles.

The detector system itself consists of two subsystems, the Scattering Neutrino Detector (SND)

*E-mail: kurbatov.phys@gmail.com
**E-mail: fedor.ratnikov@gmail.com
***E-mail: ursovharleey@mail.ru

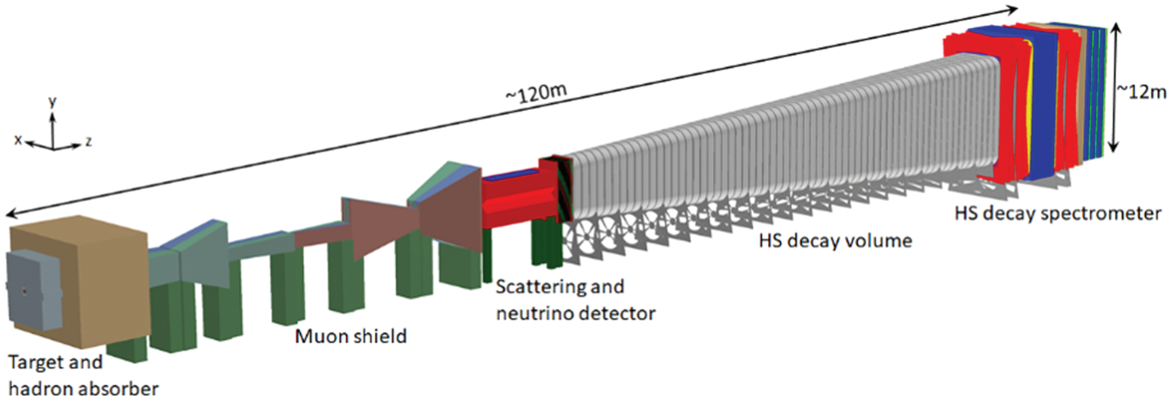

Fig. 1. SHiP experiment schema. Comprehensive Design Study 2019.

and the Hidden Sector Detector, which can register signals from hidden particles both through their decay into SM particles and by searching for signals from recoiling electrons or nuclei that have scattered off Hidden Sector particles. Figure 1 shows the layout of the experiment as of 2019. Since the publication of the initial papers discussing the main scientific goals and equipment of the SHiP experiment [1], the experiment has undergone significant changes in its detector system. In the 2019 report, a Comprehensive Design Study (CDS) [8] was presented, where a large portion of the detector system was redesigned: the geometric parameters of the decay volume were changed, some veto systems were removed, and the construction of the electromagnetic calorimeter, initially based on the “shashlik” system, was replaced.

2.1. Beam Dump Facility

The Beam Dump Facility (BDF) integrates the beam extraction area and the target along with the hadron absorber. The expected number of interactions of incident protons with the target over 5 years of operation is 2×10^{20}, with 4×10^{13} protons per second during the experiment. The target is hybrid, consisting of blocks made from an alloy of molybdenum doped with titanium and zirconium (58 cm), followed by 58 cm of pure tungsten. The choice of these materials is due to the fact that the collision of the beam with the target produces a large number of short-lived resonances, pions, and kaons, whose decay creates an enormous flux of muons and neutrinos. The target must be made of a material with a very short interaction length so that these hadrons do not have time to decay and are stopped within it. The overall dimensions of the target are 1.2 m in length with transverse dimensions of 30×30 cm^2. Behind the target, several meters of iron are placed to absorb hadrons and electromagnetic radiation from the beam-target collisions.

As a result, the expected flux of heavy mesons will be 1.6×10^{18} D-mesons and 1×10^{14} B-mesons.

2.2. Physical Program

Effective exploration of the parameter space of models introducing FIPs is only possible if background is well controlled and reduced to negligible levels. The signals from FIPs that the SHiP experiment is sensitive to can be divided into two main categories: fully and partially reconstructed decays. The first category refers to decays where there are at least two charged particles that can be detected (charged) and no invisible particles (neutrinos) that can carry away momentum. Examples include DP $\to \mu^{\pm}\mu^{\mp}$ and HNL $\to \mu^{\pm}\pi^{\mp}$. The latter category refers to decays with at least two charged particles and at least one invisible particle in the final state, such as HNL $\to \mu^{\pm}\mu^{\mp}\nu$. In all cases, the experimental signature is a reconstructible decay vertex of the FIP within the decay volume and its momentum.

As an example, a sensitivity plot of the experiment to HNL detection considering all decay channels is shown (see Fig. 2). Assuming zero background, the SHiP experiment will be able to cover a large region in the HNL parameter space.

3. SHiP MUON SHIELD

SHiP is designed as a zero-background experiment. When the beam hits the target, many secondary particles are produced. Most of these need to be removed before they reach the decay volume. The hadron absorber serves to absorb particles with large interaction cross-sections. Muon shield is a key element for removing muons, which are the primary source of background. The goal is to reduce the flux of approximately 10^{11} muons per spill by 6 orders of magnitude. Thus, on one hand, the shield must

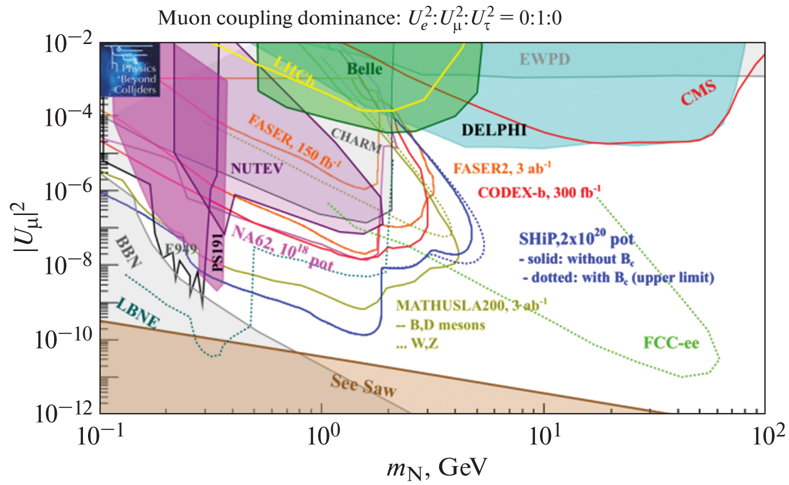

Fig. 2. The sensitivity to HNL, considering only $|U_\mu|^2$. The shaded regions represent areas excluded by existing experimental data. The solid lines indicate the potential coverage areas of future experiments. The graph is plotted with a 90% confidence interval according to the zero-background hypothesis of the experiments [7].

provide good background suppression, and on the other hand, it should not be too heavy or expensive.

For the numerical determination of the muon shield's quality, the experiment simulation is based on Geant4 with a fixed generated weighted muon sample. The primary quality metric is the number of weighted muon tracks recorded in the tracking chambers. To avoid potential problems with track reconstruction algorithms, we considered a set of hits in at least 3 out of 4 tracking stations as "reconstructed tracks." The first and last stations are mandatory. Besides shield quality, the mass of the shield is an important numerical characteristic. There are specific limitations on how heavy the entire setup can be. Additionally, the cost of the material constitutes a significant portion of the total shield cost.

The muon shield consists of 6 magnets with identical parameterization and a magnetic field of 1.7 T. The field directions are opposite for the first and second halves of the shield. The idea is to deflect high-energy muons out of the acceptance area in the first three magnets within the core, and in the subsequent magnets, within the yoke.

To define the shape of one magnet, 7 parameters are required: 3 parameters for the entrance plane, 3 parameters for the exit plane, and the length of the magnet. With 6 magnets and fixed gaps between them, we obtain 42 parameters to define the shape of the shield, as shown in Fig. 3.

4. SHiP MUON SHIELD OPTIMIZATION

Over the past year, the SHiP experiment has undergone several changes due to the consideration of new potential locations. One of these changes involves reducing the length of the muon shield from 35 to 30 m. The previously used configuration was obtained through fine optimization, and any changes inevitably lead to a significant decrease in shield performance.

The initial task was to reduce the total length of the shield from 35 to 30 m. As a first approximation, a method of uniformly reducing the length of each magnet was chosen, which led to a fourfold increase in the muon flux passing through the shield. Detailed investigation revealed two distinct spots from muon tracks in the tracking chambers. These corresponded to high-energy muon tracks that were insufficiently deflected in the first half of the shield and entered the gap between the core and yoke of magnet no. 4.

To avoid this effect, a configuration was proposed where only the last three magnets were shortened ("combi"), which significantly reduced the muon background but still did not achieve the desired levels.

Finally, a full cycle of Bayesian optimization of the shield was conducted. The objective function is

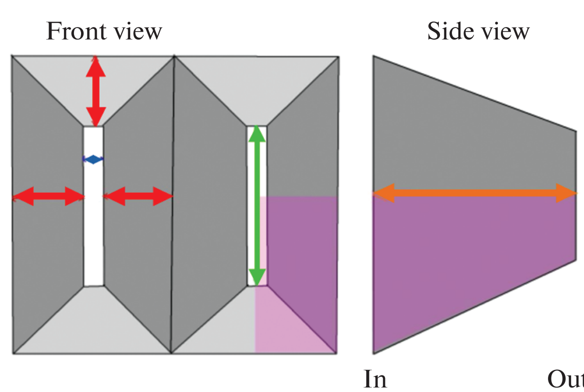

Fig. 3. Single magnet parametrization schema.

Table 1. Different shield configurations performance

Shield version	Tracking station muon flux, ($10^3\times$ muons/spill)	Shield length, m
ECN4	45	35
ECN3 combi	160	30
ECN3 optimized	67	30
ECN3 SC	22	20

represented by the formula (1):

$$F_{\text{cost}} = (1 + e^{\frac{10(M-M^*)}{M^*}}) \times (1 + \Sigma\sqrt{\frac{400-(x+200)}{400}}), \quad (1)$$

where M is the mass of the shield, M^* is a constant, and x is the x-coordinate of the muon hit on the sensitive plane. The first part of the function prevents the shield from becoming too large, while the second part reduces the muon flux. A nonlinear function of the hit coordinate instead of directly counting muons was chosen to increase the sensitivity of the optimization to minor changes in the flux.

To evaluate the loss function for a given configuration, the results of Monte Carlo (MC) simulations with a special muon sample were used as input data. The optimization sample was created based on the base sample for 1 spill of data by removing the generation stage weights and limiting the sample size for faster simulation completion.

The simplest surrogate model for Bayesian optimization is Gaussian processes (GP). Unfortunately, standard GP has $\mathcal{O}(n^3)$ computational complexity and $\mathcal{O}(n^2)$ memory complexity. This does not allow obtaining a stable result for high-dimensional optimization tasks. To address these issues, the Bayesian optimization with sparse axis-aligned subspaces (SAASBO) [9] and variational nearest neighbor Gaussian process (VNNGP) [10] approaches were used. This allowed achieving several thousand iterations in the optimization. The calculations were performed on the Yandex Cloud infrastructure [11].

In addition to optimizing the basic option with 6 warm magnets, an optimization of an alternative shield configuration was carried out, where the first 3 magnets were replaced by one superconducting magnet while maintaining the overall magnetic field integral. The optimization approaches were identical for both cases.

Also another version of FCN (see Eq. (2)) was used for the trade-off between tracking station and SND muon fluxes trade-off. a_i—some parameters, T and S—muon fluxes nonlinear functions (like in equation (1)) for Tracking stations and SND, T_{good} and S_{good}—some "good enough" values of fluxes, no need to try to make it smaller. New cost function allowed the controlled trade-off between SND and Tracking Stations muon fluxes:

$$\begin{gathered} F_{\text{cost}} = W(T_{\text{flux}} + SND_{\text{flux}} + 1), \\ W = a_1 W_{\text{sc}} + a_2 W_{\text{warm}}, \\ T_{\text{flux}} = a_3 \max(0, (T - T_{\text{good}})), \\ SND_{\text{flux}} = a_4 \max(0, (S - S_{\text{good}})). \end{gathered} \quad (2)$$

The optimization results are presented in Table 1.

5. YANDEX CLOUD INFRASTRUCTURE FOR MASSIVE COMPUTING

As one can see in the previous chapter, two types of computational resources are required to conduct such optimization: one to run the optimization cycle and another to make the Monte Carlo simulation runs to calculate the cost function for the given shield configuration.

The first one should be presented as a single machine with the at least 32 GB RAM and (in ideal case) some GPU. This allows to generate surrogates fast and for the big amount of points in the parameters space.

The configuration to run MC tasks should be different. We need to optimize the simulation time needed to obtain the cost function value for the single point. And unlike the previous task this one can be easily paralleled. Still, MC is a high cpu load task. For the optimal performance the infrastructure of the Yandex Cloud platform [11] was used. It was presented as a Kubernetes cluster with the approximately 1600 cpu available. To run the simulation all environment have been put into the Docker container. The parameters needed for simulation was passed as an environmental variables. The output of the task was saved to the Yandex Cloud S3-share. The input muon sample was loaded to the every machine in the Yandex Cloud cluster for the faster access and lower network load.

The single point task was divided into several independent jobs to process the different parts of the input muon sample in parallel.The default split was 20 jobs per point. This gave the optimal simulation time. With increasing split number too many time was needed to start the additional amount of Docker containers. So approximately 80 points could be processed simultaneously.

All tasks have been controlled from the proxy-machine of Yandex Cloud platform. The same machine was used to read output of the MC run from S3 share and calculate the cost function after all the jobs for the given configuration succeeded.

The advantage of such approach—incredibly high performance for the MC tasks and pretty flexible compatibility with any computer to be used to run the optimization loop. SSH tunnel was the only thing needed to fully control all the MC-related tasks.

6. CONCLUSIONS

BDF/SHiP provides an excellent opportunity to detect FIPs in decays of heavy quarks (or to close this "topic" experimentally). This complements the search for FIPs at the HL-LHC and the future $e+e$-collider (where FIPs can be searched for in boson decays). Bayesian optimization of the muon shield outperforms manual tweaking and yields results that satisfy the physical requirements of the experiment. The developed approach is shown to be effective for both the warm-magnet shielding variant and the superconducting configuration. The choice of cost function provides the mechanism of trade-off between SND and Tracking Stations muon fluxes.

FUNDING

This work was supported by Yandex Cloud Computing. The research leading to these results received funding under the program of the Fundamental Research Fund of the National Research University Higher School of Economics.

CONFLICT OF INTEREST

The authors of this work declare that they have no conflicts of interest.

REFERENCES

1. M. Anelli, S. Aoki, G. Arduini, J. J. Back, A. Bagulya, W. Baldini, A. Baranov, G. J. Barker, S. Barsuk, M. Battistin, J. Bauche, A. Bay, V. Bayliss, L. Bellagamba, G. Bencivenni, M. Bertani, O. Bezshyyko, D. Bick, N. Bingefors, A. Blondel, M. Bogomilov, A. Boyarsky, D. Bonacorsi, D. Bondarenko, W. Bonivento, J. Borburgh, T. Bradshaw, R. Brenner, D. Breton, N. Brook, M. Bruschi, A. Buonaura, S. Buontempo, S. Cadeddu, A. Calcaterra, M. Calviani, M. Campanelli, C. Capoccia, A. Cecchetti, A. Chatterjee, J. Chauveau, A. Chepurnov, M. Chernyavskiy, P. Ciambrone, C. Cicalo, G. Conti, K. Cornelis, M. Courthold, M. G. Dallavalle, N. D'Ambrosio, et al. (SHiP Collaboration), arXiv Preprint (2015).
https://doi.org/10.48550/arXiv.1504.04956
2. D. Banerjee, J. Bernhard, M. Brugger, N. Charitonidis, N. Doble, L. Gatignon, and A. Gerbershagen, The North Experimental Area at the Cern Super Proton Synchrotron, Technical Report CERN-ACC-NOTE-2021-0015, (CERN, Geneva, 2021).
https://doi.org/10.17181/CERN.GP3K.0S1Y
3. E. Cortina Gil, E. M. Albarrán, E. Minucci, G. Nüssle, S. Padolski, P. Petrov, N. Szilasi, B. Velghe, G. Georgiev, V. Kozhuharov, L. Litov, T. Husek, K. Kampf, M. Zamkovsky, R. Aliberti, K. H. Geib, G. Khoriauli, K. Kleinknecht, J. Kunze, D. Lomidze, R. Marchevski, L. Peruzzo, M. Vormstein, R. Wanke, A. Winhart, M. Bolognesi, V. Carassiti, S. Chiozzi, A. C. Ramusino, A. Gianoli, R. Malaguti, P. Dalpiaz, M. Fiorini, E. Gamberini, I. Neri, A. Norton, F. Petrucci, M. Statera, H. Wahl, F. Bucci, R. Ciaranfi, M. Lenti, F. Maletta, R. Volpe, A. Bizzeti, A. Cassese, E. Iacopini, A. Antonelli, E. Capitolo, C. Capoccia, et al., J. Instrum. **12**, P05025 (2017).
https://doi.org/10.1088/1748-0221/12/05/P05025
4. W. Buchmüller and C. Lüdeling, arXiv Preprint (2006).
https://doi.org/10.48550/arXiv.hep-ph/0609174
5. P. Langacker, *The Standard Model and Beyond* (CRC Press, 2017).
https://doi.org/10.1201/b22175
6. P. Agrawal, M. Bauer, J. Beacham, A. Berlin, A. Boyarsky, S. Cebrian, X. Cid-Vidal, D. D'enterria, A. De Roeck, M. Drewes, B. Echenard, M. Giannotti, G. F. Giudice, S. Gninenko, S. Gori, E. Goudzovski, J. Heeck, P. Hernandez, M. Hostert, I. G. Irastorza, A. Izmaylov, J. Jaeckel, F. Kahlhoefer, S. Knapen, G. Krnjaic, G. Lanfranchi, J. Monroe, V. I. M. Outschoorn, J. Lopez-Pavon, S. Pascoli, M. Pospelov, D. Redigolo, A. Ringwald, O. Ruchayskiy, J. Ruderman, H. Russell, J. Salfeld-Nebgen, P. Schuster, M. Shaposhnikov, L. Shchutska, J. Shelton, Y. Soreq, Y. Stadnik, J. Swallow, K. Tobioka, and Y.-D. Tsai, Eur. Phys. J. C **81**, 1015 (2021).
https://doi.org/10.1140/epjc/s10052-021-09703-7

7. J. Beacham, C. Burrage, D. Curtin, A. De Roeck, J. Evans, J. L. Feng, C. Gatto, S. Gninenko, A. Hartin, I. Irastorza, J. Jaeckel, K. Jungmann, K. Kirch, F. Kling, S. Knapen, M. Lamont, G. Lanfranchi, C. Lazzeroni, A. Lindner, F. Martinez-Vidal, M. Moulson, N. Neri, M. Papucci, I. Pedraza, K. Petridis, M. Pospelov, A. Rozanov, G. Ruoso, P. Schuster, Y. Semertzidis, T. Spadaro, C. Vallée, and G. Wilkinson, J. Phys. G: Nucl. Part. Phys. **47**, 010501 (2020). https://doi.org/10.1088/1361-6471/ab4cd2
8. C. Ahdida et al. (SHiP Collaboration), SHiP Experiment—Comprehensive Design Stidy Report CERN-SPSC-2019-049, SPSC-SR-263 (CERN, Geneva, 2019). https://cds.cern.ch/record/2704147.
9. D. Eriksson and M. Jankowiak, Proc. Mach. Learn. Res. **161**, 493 (2021).
10. L. Wi, G. Pleiss, and J. P. Cinningham, Proc. Mach. Learn. Res. **162**, 24114 (2022).
11. Yandex Cloud. https://cloud.yandex.ru/.